Influence of Processing Conditions in Small-Scale Melt Mixing and Compression Molding on the Resistivity and Morphology of Polycarbonate–MWNT Composites

Gaurav Kasaliwal, Andreas Göldel, Petra Pötschke

Department of Polymer Reactions and Blends, Leibniz Institute of Polymer Research Dresden, 01069 Dresden, Germany

Received 9 July 2008; accepted 21 December 2008
DOI 10.1002/app.29930
Published online 6 March 2009 in Wiley InterScience (www.interscience.wiley.com).

ABSTRACT: Polycarbonate (PC) composites containing 1 wt % multiwalled carbon nanotubes (MWNT) were produced in a small-scale DACA microcompounder under variation of mixing temperature and mixing speed at fixed mixing time according to a two-factor and three-level factorial design. The extruded strands were compression molded under comparable conditions, and their volume resistivity values indicated differences of about 14 orders of magnitude as well as big differences in the state of MWNT agglomerate dispersion (evaluated as macrodispersion index) are observed. The results indicate that mixing at high melt temperature and high speed can lead to the composites having low resistivity and high dispersion index at low mixing energy input. The influence of compression molding parameters was investigated on precompounded PC composites containing 1 and 2 wt % MWNT. Compression molding parameters such as temperature, time, and speed were varied according to a three-level and three-factor factorial design. By adjusting compression molding parameters, the volume resistivity of PC with 1 wt % MWNT composites can be varied over eight orders of magnitude, whereas for 2 wt % MWNT, the variation was within one decade. The electrical volume resistivity results indicate the highest influence of the compression molding temperature followed by time. © 2009 Wiley Periodicals, Inc. J Appl Polym Sci 112: 3494–3509, 2009

Key words: polycarbonates; nanocomposites; multiwalled carbon nanotubes; compounding; electrical resistivity

INTRODUCTION

The extraordinary characteristic of carbon nanotubes (CNT)[1–3] such as electrical conductivity, mechanical strength, thermal conductivity in combination with their high aspect ratio, and low density makes them lucrative fillers in polymers especially for conductive polymers and electrostatic dissipative applications. Thus, polymer–CNT nanocomposites find a number of high-end applications, for instance, in Li-ion batteries,[4] polymeric solar cells, proton exchange membrane fuel cells,[5] photovoltaic devices,[6] thermoionic emitters, electrochemical sensors,[7–9] flat panel display screens,[10] as well as electromagnetic interference-shielding (EMI-shielding),[11–13] microwave absorbing,[14] and electrostatic charge dissipation (ESD)[15,16] materials.

In the manufacture of electrically conductive or electrostatic dissipative polymer composite materials, carbon black (CB) is the preferred conventional filler. However, such polymer composites normally need high loadings of carbon black or any other conductive filler, which in turn may harm the mechanical properties of the matrix polymer. In contrast to conventional fillers like CB, CNT are required in very low quantities to achieve electrical percolation because of their very high aspect ratio. Additionally, they can also mechanically reinforce the polymer composite, enhance thermal conductivity and fire retardancy, or contribute to improvements in tribological properties. Because of the steady lowering of their prices, multiwalled carbon nanotubes (MWNT) become increasingly important for the production of high-quality conductive or electrostatic dissipative polymer composites. Polycarbonate (PC) is a versatile engineering thermoplastic with a wide range of useful properties. Manufacturing of PC–MWNT nanocomposites as pure material or in blends is of commercial importance, as they can be potentially used, e.g., in housing applications, parts to be electrostatically painted, and helmets.

For the production of polymer–MWNT nanocomposites on industrial scale, melt processing represents an economically suitable cheap method to produce large volumes of industrial and consumer products. In addition, it enables the use of existing manufacturing technology for filled thermoplastic

Correspondence to: P. Pötschke (poe@ipfdd.de).
Contract grant sponsor: German Federal Ministry of Education and Research (BMBF); contract grant number: 02PU2392.

composite products. However, the performance of polymer–CNT composites is greatly influenced by the extent of nanotube dispersion and individualization in the polymer matrix. In this context, the shear forces present in the mixing equipment during melt processing can help to disperse and distribute primary MWNT agglomerates in the polymer matrix. To evaluate the general effects of different melt-processing parameters on the state of nanotube dispersion in a polymer matrix small-scale melt mixing can be adapted as a fast and efficient method requiring low sample amounts. It can be assumed that deduced basic relationships may be adapted to a certain extent also toward larger industrial extruders especially when regarding basic mechanisms of distribution and dispersion.

Manufacturing of PC–MWNT nanocomposites by melt mixing using the masterbatch dilution method or direct incorporation of MWNT in PC has been extensively discussed in the literature[17–23]; however, without the focus and detailed investigation of the influence of mixing conditions as it is the aim of this study. Pötschke et al.[21] used a twin-screw extruder to dilute a masterbatch and found electrical percolation between 1 and 2 wt % MWNT. A variation in small-scale mixing conditions during masterbatch dilution is described,[22] where depending on the screw speed and mixing time either conductive or insulating composites of 1 wt % MWNT are reported. Pegel et al.[18] illustrate on transmission electron microscopy (TEM) images the influence of mixing temperature and mixing speed in composites with 0.875 wt % MWNT produced by small-scale masterbatch dilution on the nanotube dispersion and secondary agglomeration. Lin et al.[19] studied PC–MWNT composites prepared by different small-scale melt-mixing equipments and concluded from TEM investigations the best dispersion of MWNT aggregates when using a DACA microcompounder. Nevertheless, when compared with the other mixers, a higher content of MWNT was needed to achieve rheological and electrical percolation.

This article deals in its first part with the influence of processing conditions during small-scale melt mixing by direct incorporation of MWNT in PC on electrical volume resistivity and MWNT dispersion, which was assessed using a macrodispersion index based on the remaining primary agglomerate area. A systematic investigation was made using a statistical factorial experimental design to find the most influencing conditions or combination of conditions for electrical volume resistivity and dispersion index. A MWNT concentration near the electrical percolation threshold was selected, and then mixing temperature and mixing speed were varied according to a three-level and two-factor factorial design, while mixing time was kept constant. In addition, the effect of two different mixing conditions (optimized and nonoptimized) on the percolation threshold of MWNT in PC is also investigated. The results were correlated to the mixing energy input. Such a correlation was presented by Krause et al.[24] for melt-compounded PA6 nanocomposites containing 5 wt % MWNT, where by varying the mixing time and mixing speed, a minimum in electrical resistivity at a particular mixing energy input was found. Further increase in mixing energy led to better dispersion of the nanotubes, but electrical resistivity increased drastically.

To characterize the electrical and mechanical properties of polymer composites, a subsequent shaping process is required. Next to injection molding, especially for small-scale mixing, the manufactured polymer composites are compression molded to form defined geometries such as plates. Although detailed studies on the influence of injection molding conditions on resistivity/conductivity were presented recently for PC-MWNT composites,[23,20] not much attention is paid on the effect of compression molding conditions. Pegel et al.[18] discussed the effect of two different pressing temperatures and speeds on dielectric spectra of PC-0.875 wt % MWNT composites. They illustrated that for the same composite depending on the compression molding conditions either percolated or nonpercolated systems can be obtained and attributed to an increase in conductivity to secondary agglomeration of dispersed MWNT in the polymer melt. Recently, Grossiord et al.[25] investigated the effect of compression molding conditions on the percolation threshold of composites prepared by surfactant-assisted MWNT dispersion in polystyrene latex. They found that by increasing compression molding temperature and time, the percolation threshold of their system was reduced because of the better diffusive motion of MWNT inside the PS latex particles. However, the influence of various compression molding conditions on electrical volume resistivity of melt-compounded polymer–MWNT composites has not been systematically investigated so far in literature. In the second part of this work, melt-compounded PC–MWNT composites near the percolation threshold concentration (PC + 1 wt % MWNT) and above percolation threshold concentration (PC + 2 wt % MWNT) were used to comprehensively investigate the influence of compression molding conditions on volume resistivity using a three-level and three-factor factorial design. The compression molding conditions such as pressing temperature, pressing time, and pressing speed were varied.

MATERIALS AND EXPERIMENTAL

Materials

The MWNT used in this work (Baytubes® C150HP, Bayer MaterialScience AG, Leverkusen, Germany)

are produced by CVD process and were supplied as agglomerates. The carbon purity of this highly purified material is > 99%, the outer mean nanotube diameter is reported to be in the range of 13–16 nm, the length of the tubes is less than 10 μm, and their bulk density is 140–230 kg/m^3.[26]

As PC, Makrolon 2600 (Bayer MaterialScience AG, Leverkusen, Germany), an injection molding grade with a medium viscosity (MVR 12.5 cm^3/10 min) and a density of 1.2 g/cm^3 was selected.

For investigation of the influence of compression molding conditions, MWNT precompounded in PC using twin-screw extrusion were used. The PC composites contained 1 and 2 wt % MWNT and were supplied by Bayer MaterialScience AG.

Before mixing or pressing, PC and PC–MWNT composites were dried at 90°C and MWNT were dried at 120°C overnight under vacuum.

Melt compounding

A DACA Microcompounder (DACA Instruments, Goleta, CA), a small-scale laboratory compounder with a volume of 4.5 cm^3, was used to melt-mix the PC–MWNT nanocomposites. It is a conical, corotating twin-screw microcompounder with a bypass in which mixing parameters such as mixing temperature, mixing speed, and mixing time can be easily controlled and torque values can be monitored.

Predried PC and MWNT were added simultaneously in 2–3 charges into the running microcompounder in about 2.5 min. Since the electrical percolation threshold of MWNT in PC was found to be near 1 wt % content in earlier investigations,[22,27] in a first set of compounding experiments, the influence of mixing conditions on electrical volume resistivity was investigated at 1 wt % MWNT addition. For this purpose, a two-factor and three-level factorial experimental plan was used. Two important processing factors, namely, mixing speed and mixing temperature, were varied keeping the mixing time constant. Three different levels (low, medium, and high) of mixing temperature (set barrel temperature) and rotor speed were used as indicated in Table I leading to nine experiments. Considering the general residence time of polymers in an industrial extruder, the mixing time was kept constant at 5 min. After mixing, the extruded material was taken out as a strand (diameter ~ 2 mm) using the set screw speed through the heated cylindrical die into air without additional cooling or drawing.

For the determination of electrical percolation threshold of Baytubes® C150HP in PC in the second set of compounding experiments, composites containing 0.5, 1, 1.5, 2, 2.5, and 3 wt % MWNT in PC were made using two different mixing conditions. First, nonoptimized mixing conditions were used (265°C barrel temperature, 50 rpm rotor speed), and secondly after performing the variation in mixing conditions those leading to the highest macrodispersion were applied (280°C barrel temperature, 200 rpm rotor speed), whereas in both case mixing time was kept at 5 min.

TABLE I
Mixing Conditions Used in the DACA Microcompounder

Factors	Temperature (°C) (*A*)	Speed (rpm) (*B*)
High level	260	50
Medium level	280	100
Low level	300	200

The mixing energy E (in J) introduced during composite processing was calculated using the following equation:

$$E = \int_0^t P dt = \int_0^t N \cdot 2\pi \cdot \tau dt$$

Here, P is the engine output dependent on the time, N is the rotation speed in revolution per minutes (rpm), τ is the torque, which was measured time dependent during the mixing process (in Nm), and t is the mixing time (in min). The specific mixing energy (in J/cm^3) was calculated for the volume of the microcompounder of 4.5 cm^3.

Compression molding of plates

Compression molding procedure

Compression molding of plates was performed using a Weber hot press (Model PW 40 EH, Paul Otto Weber GmbH, Remshalden, Germany). In this press, pressing temperature, pressing time, and pressing speed can be controlled. To get good quality bubble-free plates, a pressing procedure was developed. A square metallic (brass) frame of dimensions 80 mm × 80 mm and 1-mm thickness was used for the precompounded composites, whereas for materials obtained from DACA Microcompounder (due to less quantity), a circular frame of diameter 60 mm and thickness 0.5 mm was used. A polyimide separating film and a brass plate on each side of the frame were used to support the material and enabling separation of the sample from the brass plates. An additional pair of iron plates is used to prevent the composite melt spillage on hot press. The PC–MWNT composite in the shape of granules or about 1–2 cm long pieces of extruded strands was placed inside the frame. The material is

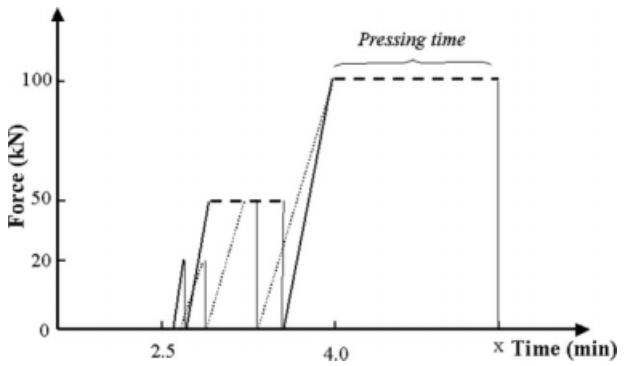

Figure 1 Procedure describing compression molding illustrating stepwise increase of force corresponding to pressing time (only for explanation, not drawn with scale), full line represents 95 or 50 mm/min and dotted line represents 6 mm/min pressing speed.

then evenly spread in the central part of the frame. Another polyimide film and corresponding brass and iron plates are placed over the frame. The frame and plates were placed inside the hot press, and the press was closed so that both the hot-press plates (upper and lower) are in contact with the iron plates. A stable desired temperature is obtained in initial 2.5 min and a uniform composite melt is produced. The force on the press plates, during this time, is between 0 and 2 kN. After initial 2.5 min, the press is opened by moving away the upper hot plate by a certain distance (ca. 4 mm), and then the press is again closed with the defined pressing speed. To uniformly fill the entire frame with the polymer melt and to remove the air bubbles, the force on the plates is then increased stepwise in next 1.5 min (as shown in Fig. 1). The force is increased from 0 to 20 kN and then released. In the next step, the force is again increased from 0 to 50 kN and then again released. Depending on the pressing speed, the material is hold at 50 kN force for different time. Before the end of fourth minute, finally, the applied force is again increased to 100 kN. Force release was performed to enable gassy material to get out from the melt to obtain bubble-free plates. Please note that pressing time is the time for which the material is pressed at full force of 100 kN (see Fig. 1).

After the required pressing time is completed, the sample was removed from the press and cooled down immediately using chilled plates (−5 to 10°C) so as to freeze the internal morphology of the pressed plate.

For materials obtained from DACA Microcompounder, a press temperature of 265°C, a pressing speed of 6 mm/min, and a pressing time of 1 min were applied so as to minimize any effects arising from the compression molding conditions on electrical resistivity. For premixed composites, the conditions were varied as discussed later.

Compression molding experiments using a factorial experimental design

To study the influence of compression molding conditions on electrical resistivity of plates, a three-factor and three-level factorial experimental design was performed using compression molding conditions as described in Table II, resulting in 27 experiments.

In each compression molding experiment, ~ 8 g of precompounded composites of PC with 1 or 2 wt % MWNT were used. In case of PC, general processing temperature is recommended in the range of 260–300°C. For pressing experiments, three temperatures, namely 260, 280, and 300°C, were set as adjusted stage temperatures so that the complete processing temperature range can be investigated. The pressing speeds were selected by dividing the maximum speed achievable by our press in three equal intervals, which were 6, 50, and 95 mm/min. The pressing speed is the speed with which lower hot stage moves toward the upper hot stage during the closing of press. It influences the characteristic squeeze flow inside the material but also the holding time at 50 kN during the stepwise increase of force. Pressing time is the time for which the material is pressed at full force of 100 kN (see Fig. 1), and pressing times of 1, 4, and 7 min are chosen. Referring to Figure 1, it should be noted that the total compression molding time is always 4 min higher than the specified pressing time, ensuring complete melt formation.

Specimen characterization

Volume resistivity measurement

The electrical volume resistivity of the PC–MWNT composite samples is measured depending upon their resistivity values. For high resistivity samples (resistivity $> 10^7$ Ω cm), a Keithley Electrometer 6517A with an 8009 Resistivity test fixture equipped with ring electrodes was used. For samples having lower volume resistivity, the measurements were performed on strips cut from the pressed sheets using a four-point test fixture combined with a Keithley Multimeter DMM 2000. The four-point test fixture has gold contact wires with a distance of 16 mm between the source electrodes and 10 mm between the measuring electrodes.

TABLE II
Compression Molding Conditions

Factors	Pressing temperature (°C) (*A*)	Pressing speed (mm/min) (*B*)	Pressing time (min) (*C*)
High level	300	95	7
Medium level	280	50	4
Low level	260	6	1

The volume resistivity was measured at 24°C and 40% relative humidity. Prior to measurements, the surfaces of the samples were cleaned with ethanol. For each specimen, two measurements were made for the high resistivity samples, and four measurements were made for the low resistivity samples.

Optical microscopy

The morphology of extruded strands and pressed plates was studied by means of optical microscopy. Thin sections of 20 μm thickness were prepared perpendicular to the extrudate or plate direction on a RM 2055 microtome (Leica, Wetzlar, Germany) at room temperature. A glass knife with a cut angle of 35° was used. Light transmission microscopy was performed on these thin sections using 10× objective magnification, the micrographs were imaged with an Olympus BX2 microscope equipped with a camera DP71 considering the entire cross-sectional area.

Using such micrographs, the CNT macrodispersion was quantified. This method is similar to that known in rubber industry as "undispersed carbon black" or "undispersed silica white" measurements and was described by Stumpe and Railsback[28] and modified by Le et al.[29] To evaluate the dispersion of MWNT, a similar method as described elsewhere[30,31] was used. The macrodispersion index D was calculated from the area of agglomerates related to the micrograph area (A/A_0) using the following formula:

$$D = \left(1 - f\frac{A/A_0}{\nu}\right) \times 100\%$$

Here, f is a factor related to the effective volume of the filler. For CB, $f = 0.4$ has been proposed by Medalia,[32] and for CNT, $f = 0.25$ is considered by referring.[30,31] The value ν is the filler volume in % (density assumed 1.75 g/cm^3). A/A_0 is the ratio of area of agglomerates (with size >1 μm^2) to the total area in % ($A_0 = \sim 0.6$ mm^2 per micrograph). For 1 wt % MWNT, if the value of A/A_0 exceeds 2.75%, the macrodispersion index D is assumed as zero indicating the worse state of dispersion. A dispersion index of 100% means that no agglomerates of size larger than 1 μm^2 can be found indicating the best state of dispersion. For each sample, i.e., extruded strand (or pressed plate), at least six images were taken from at least four different positions along the length of the strand.

Transmission electron microscopy

TEM was performed with the help of a Philips Tecnai 20 FEG analytical electron microscope on thin sections cut at room temperature from either extruded strands (perpendicular to extrusion direction) or compression-molded plates (cross-sectional).

Rheological investigations

The viscosity of neat PC melt was measured using an ARES oscillatory rheometer (Rheometric Scientific Inc., Piscataway, NJ) at 260, 280, and 300°C under nitrogen atmosphere applying parallel-plate geometry (plate diameter of 25 mm, gap of 1–2 mm). Frequency sweeps were carried out between 100 and 0.1 rad/s using strains within the linear viscoelastic range.

Statistical analysis

For statistical analysis of the experiments performed using factorial experimental designs, the STATGRAPHICS PLUS statistical software was applied. For the analysis, the macrodispersion index D and logarithmic values of the measured volume resistivity in Ohm cm ($\log_{10}$ resistivity) were used. By fitting the processing parameters (variables) and experimental results, regression equations were generated. In the regression equations, which are mentioned here, only the main factors are incorporated. The analysis of variance (ANOVA) was used to calculate the correlation coefficient R^2. Estimated response surface charts[33] of the experimental results indicating measured value and the model plane fitted by using the regression equations are shown as they reflect the general trend of result in correlation with processing conditions. Pareto charts[34] illustrating the standardized effects are used to distinguish between factors and interaction factors with and without statistical significance to the process or experimental design under investigation. It displays the absolute values of the effects along with a reference line. Any factor or factor combination that extends beyond this reference line is considered potentially important.[35]

RESULTS AND DISCUSSION

Variations of processing conditions in melt mixing

The compounding experiments were carried out using a statistical experimental plan with two factors (mixing speed and temperature) and three levels at a fixed mixing time of 5 min. The zero shear viscosity of neat PC melt as measured at the three processing temperatures as considered in the experimental plan was found to decrease from 1710 Pa s at 260°C to 690 Pa s at 280°C and 460 Pa s at 300°C.

The volume resistivity values of composites prepared at different mixing conditions versus the mixing speed are shown in Figure 2; in addition, a point obtained at 265°C and 50 rpm is added. Depending

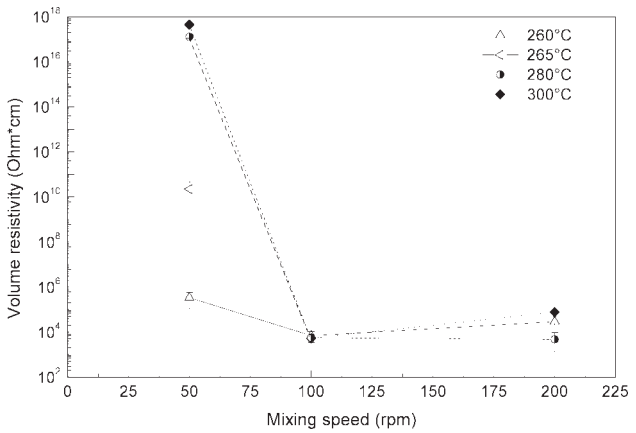

Figure 2 Volume resistivity versus mixing speed at different mixing temperatures.

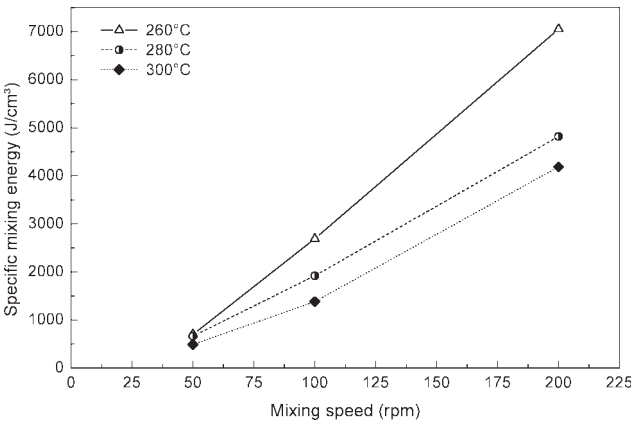

Figure 3 Specific mixing energy in dependence on mixing speed at different temperatures.

on the mixing conditions, the difference in the electrical volume resistivity values was found to be as high as 14 orders of magnitude. The mixing energy introduced in the system at different temperatures and mixing speeds is shown in Figure 3. An increase in mixing speed and lowering of melt temperature result in higher torque values and thereby leads to increasing mixing energy.

In Figure 2, it is clearly seen that composites prepared at high mixing temperature and low mixing speed show resistivity values similar to pure PC (10^{17} Ω cm) and are electrically not percolated. The sample prepared at 265°C and 50 rpm is at the percolation composition. All other samples are percolated and only small differences up to two decades are seen between different processing conditions. Up to 100 rpm mixing speed, the resistance decreases at all mixing temperatures considered here, whereas further increase of mixing speed to 200 rpm induced a slight increase in resistivity.

The correlation between the volume resistivity and the mixing energy at different processing temperature is shown in Figure 4.

Interestingly, this plot indicates a plateau in electrical resistivity starting at a certain specific mixing energy of about 1400 J/cm^3. The resistivity drops sharply when increasing the mixing energy up to this value, however enhancing the energy input by either reducing mixing temperature or increasing mixing speed does not change the resistivity much but a marginal increase is observed. In previous investigations on PA6 composites with 5 wt % MWNT, a minimum in resistivity was reported by Krause et al.[24] at a mixing energy of about 1800 J/cm^3; by further enhancing the mixing energy, the resistivity values increased. This indicates that a certain mixing energy is necessary to obtain a state of dispersion of MWNT leading to low resistivity values.

The percolation network formation responsible for low resistivity values is strongly connected with the dissolution of primary agglomerates and a good dispersion and distribution of the CNT. Agglomerates not dispersed during the mixing procedure reduce the amount of individualized MWNT available for the network formation.

The transformation of primary agglomerates into well-dispersed nanotubes can be imagined as a combination of different processes, which run parallel to each other. During melt mixing, the molten polymer first wets all the available surface area of the MWNT agglomerates. Wetting of MWNT is assumed to be a comparatively fast process; however, wetting quality depends on the interfacial energy between nanotubes and the polymer melt. Good wetting is a prerequisite for polymer infiltration inside the primary agglomerates. Because of the shear forces present in the compounder, MWNT agglomerates are immediately broken up into smaller MWNT aggregates, creating new surface area, which is again wetted by the polymer melt immediately. This process proceeds as long as the shear stresses that are transferred on the

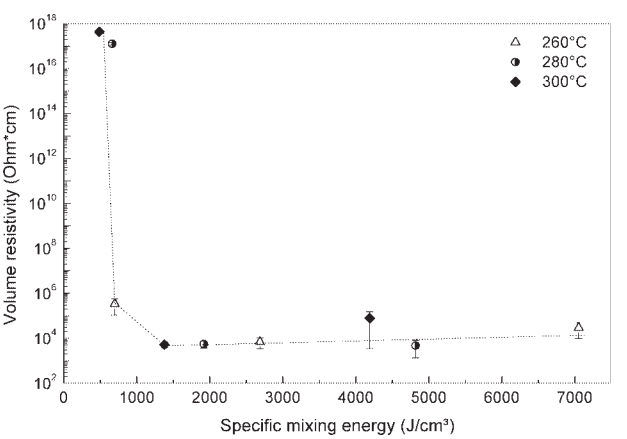

Figure 4 Volume resistivity versus specific mixing energy at different mixing temperatures.

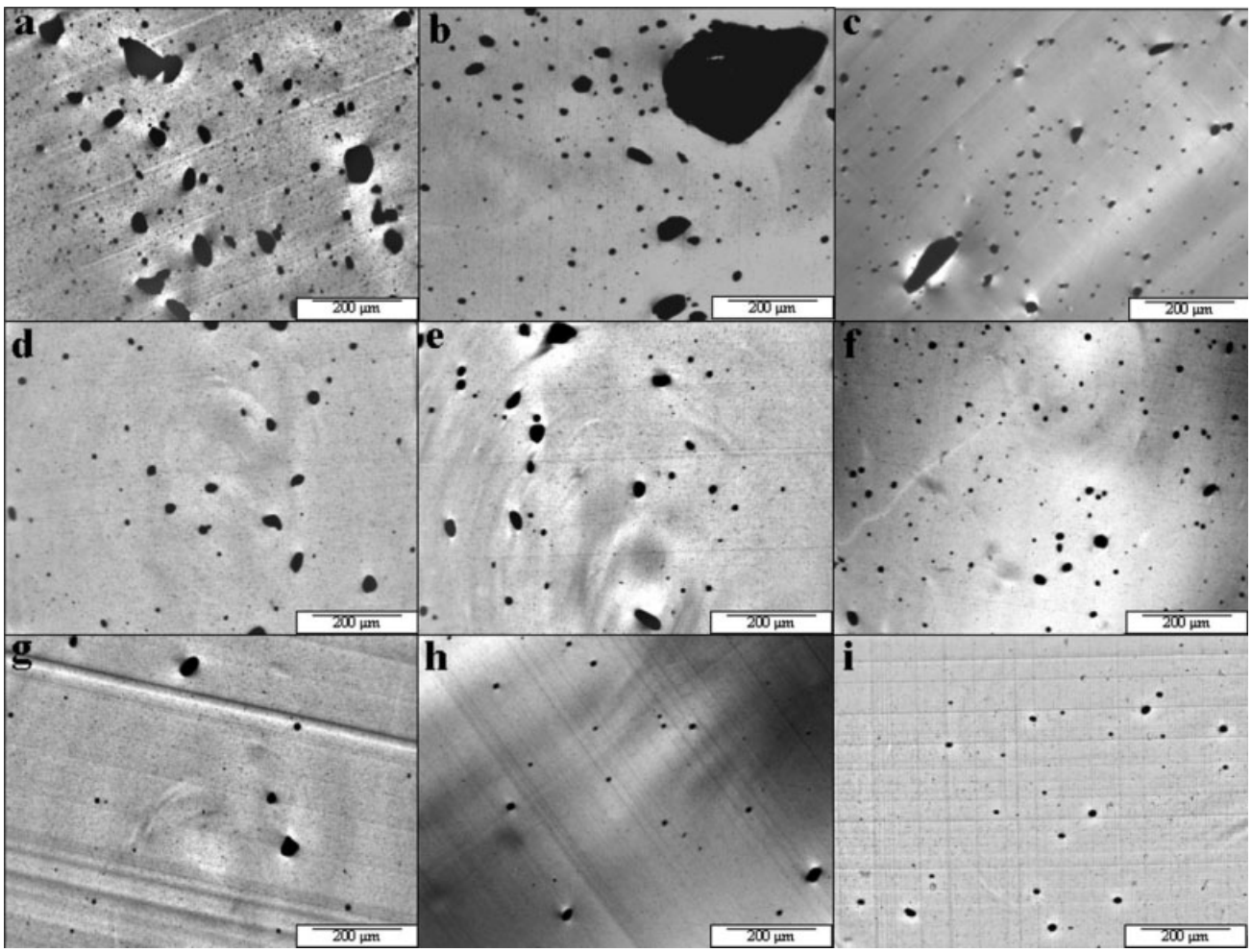

Figure 5 Optical micrographs showing dispersion of MWNT in polycarbonate at different mixing conditions: (a) 300°C, 50 rpm; (b) 280°C, 50 rpm; (c) 260°C, 50 rpm; (d) 300°C, 100 rpm; (e) 280°C, 100 rpm; (f) 260°C, 100 rpm; (g) 300°C, 200 rpm; (h) 280°C, 200 rpm; and (i) 260°C, 200 rpm.

agglomerates are higher than the shear strength of the agglomerates themselves. In the mean time, MWNT aggregates start getting distributed in the polymer melt. Thus, depending on the shear forces acting on the aggregates, a certain minimum size can be achieved by shearing, and in parallel, the newly formed smaller aggregates get again infiltrated by the polymer chains. With the infiltration of polymer chains, smaller MWNT aggregates can be broken more easily into clusters and individual MWNT. In addition, polymer melt erodes MWNT agglomerates; thereby nanotubes are separated from its surface, which are distributed within the matrix. The processes of wetting, infiltration, and erosion are strongly enhanced at lower polymer viscosity and, therefore, can be enhanced with increasing melt temperature and mixing speed. On the other hand, by having high melt viscosities combined with high shear rates, the shear stresses acting on agglomerates can be increased. In this context, it has to be mentioned that nanotube breakage during mixing may also not be excluded[36] especially if shear stresses are very high. Such breakage may reduce the aspect ratio of the nanotubes thus leading to higher electrical percolation concentrations and higher resistivity values at a given nanotube concentration. This influence was not investigated here since we did not succeed in separating tubes out of the processed samples in a way that the length could be measured.

Optical micrographs of the composites are presented in Figure 5, from which the state of macrodispersion was quantified by calculating the macrodispersion index D from the ratio of agglomerate to sample area as described earlier (Figs. 6 and 7). For selected samples, TEM micrographs are shown in Figure 8. The dependence of the macrodispersion index D on mixing speed at different temperatures as illustrated in Figure 7 shows a linear increase with mixing speed irrespective of mixing temperatures. Our results indicate that at high mixing temperatures (280 and 300°C) and low mixing speed (50 rpm), the shear stresses generated inside

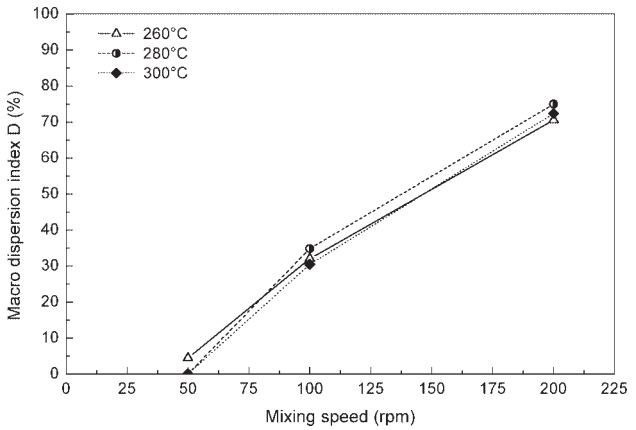

Figure 6 Macrodispersion index *D* in dependence on processing conditions.

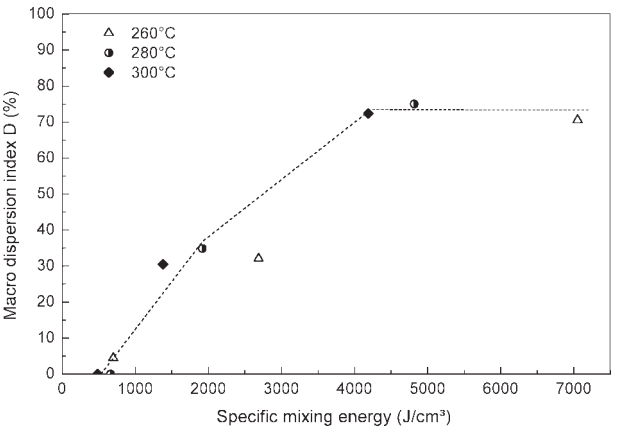

Figure 7 Macrodispersion index *D* versus specific mixing energy at different mixing temperatures.

the compounder are too low to break the primary agglomerates efficiently and erosion is probably too weak to separate enough tubes for the formation of an electrical network. Thus, there is a poor dispersion consisting of quite big MWNT aggregates, clusters, and only some individual MWNT [see Fig. 5(a,b) for 300 and 280°C, respectively] resulting in the very high electrical resistivity values. For these composites, the macrodispersion index is found to be zero as shown in Figure 6. Nondispersed agglomerates next to only very few dispersed nanotubes can also be seen in the TEM micrograph shown in Figure 8(a). From Figure 4, it can be seen that the mixing energy inputs at these temperatures were slightly lower than that at 260°C. In comparison to this, at 260°C and 50 rpm mixing speed, the shear stresses are just high enough to break the primary agglomerates into smaller aggregates [see Fig. 5(c)], which are further eroded forming an electrical network, and therefore volume resistivity is reduced considerably. The macrodispersion index is found to be around 4% (Fig. 6), and in the TEM micrograph [Fig. 8(b)], smaller nondispersed aggregates next to a higher amount of dispersed MWNTs can be seen. However, the existence of remaining agglomerates and their relatively dense inner structure suggest that polymer chain infiltration and erosion of MWNT agglomerates from their surfaces was hindered because of much higher melt viscosity and restricted further reduction in the size of MWNT agglomerates. At 100 rpm mixing speed, the volume resistivity was reduced significantly when compared with 50 rpm (Fig. 2), and all composites were conductive having similar resistivity values irrespective of the processing temperature. At the same time, the dispersion was enhanced significantly resulting in smaller agglomerates [Fig. 5(d–f)]. The macrodispersion index *D* increased up to 30% for 300°C mixing temperature and to about 32 and 35% for 260 and 280°C, respectively (see Fig. 6). Under these mixing conditions, obviously in all cases, sufficient shear stresses were generated for breakdown of agglomerates into smaller aggregates, and at the same time, the infiltration of polymer chains into small MWNT agglomerates and erosion of MWNT from agglomerate surfaces took place. In context with the quite different mixing energy inputs at the different mixing temperatures, it may be assumed that at low mixing temperature (260°C), dispersion is more pronounced by agglomerate breakage, whereas at high temperature (280 and 300°C), dispersion is predominated by

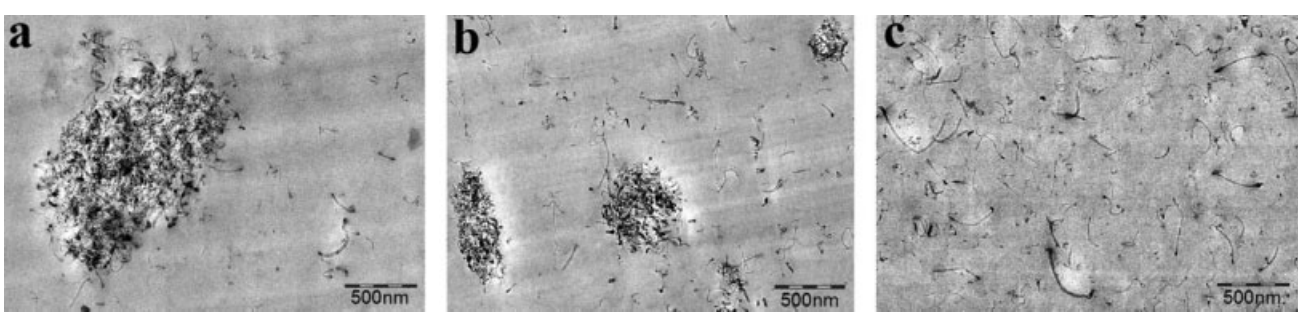

Figure 8 TEM micrographs showing dispersion of MWNT in polycarbonate at different mixing conditions: (a) 280°C, 50 rpm; (b) 260°C, 50 rpm; and (c) 280°C, 200 rpm.

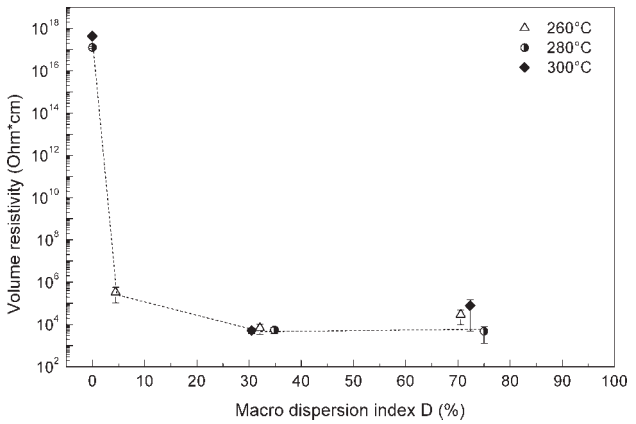

Figure 9 Volume resistivity versus macrodispersion index *D*.

wetting and infiltration of polymer chains into MWNT aggregates followed by erosion processes.

For composites prepared at 200 rpm mixing speed, a slight increase in the resistivity when compared with 100 rpm was found for samples mixed at 260 and 300°C, whereas that of the sample mixed at 280°C remained nearly constant. The size and number of MWNT agglomerates are reduced considerably when compared with 100 rpm as seen in optical micrographs [Fig. 5(g–i)]. The macrodispersion index improves drastically to 70, 72, and 75% at 260, 300, and 280°C, respectively (see Fig. 6). The TEM micrograph of the composite prepared at 280°C and 200 rpm [Fig. 8(c)] indicates a very good dispersion and distribution of MWNT with a much higher amount of dispersed tubes than seen at lower mixing speed. Under these conditions, a good balance between the dispersion by agglomerate shearing/rupture and dispersion by erosion seems to be achieved. The slight resistivity increase might be caused by tube shortening and reduction in aspect ratio; however, this was not investigated in our study.

In Figure 7, the change in macrodispersion index in dependence on the mixing energy is shown indicating increase in dispersion index with mixing energies up to $\sim$ 4000 J/cm^3 and reaching a plateau at about 70–75% with further increase in mixing energy.

According to these investigations, the best quality of CNT macrodispersion (highest value of macrodispersion index *D*) combined with the lowest value of volume resistivity is observed for the mixing conditions of 280°C and 200 rpm (energy input 4800 J/cm^3). Nearly the same low value of resistivity was achieved for 300°C and 100 rpm (energy input 1400 J/cm^3, see Fig. 4); however, here the dispersion index is significantly lower (30%).

Plotting the volume resistivity versus the macrodispersion index (Fig. 9) revealed that a certain grade of dispersion (in this case $\sim$ 30%) is needed to get low resistivity values but further increase in dispersion index does not decrease the resistivity anymore. No correlation is observed between the resistivity and dispersion indices above this certain grade of dispersion. The combination of low dispersion index with low resistivity values implies a network structure rather consisting of microsized nanotube agglomerates connected by separated nanotubes, as described elsewhere[37] than nicely dispersed tubes. However, for most applications along with low resistivity, good mechanical properties are also required, which may be negatively affected by such remaining agglomerates.

In our investigation, the maximum dispersion index reached was only 75%, which may be related to the agglomerated state of the Baytubes® material and the selected restriction to a mixing time of 5 min. This implies that especially the infiltration of polymer chains into the quite compacted primary Baytubes® agglomerates has to be improved, e.g., by enhanced mixing time. Also, using a masterbatch step may be helpful in enhancing dispersion. Toward melt mixing in industrial scale using extruders, it may be favorable to use high rotation speed and a screw profile enabling a relatively high

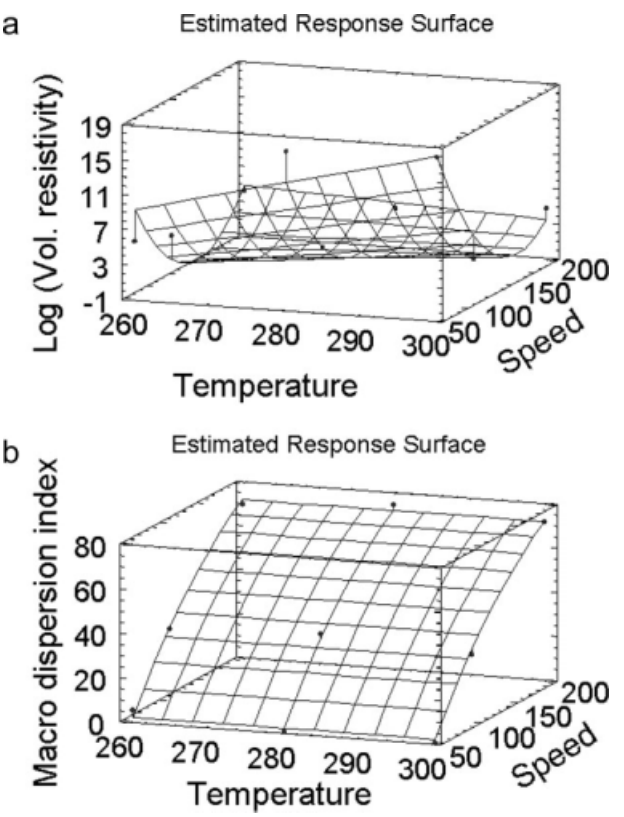

Figure 10 Estimated response surface chart of (a) log (volume resistivity) and (b) macrodispersion index *D* in correlation to mixing conditions.

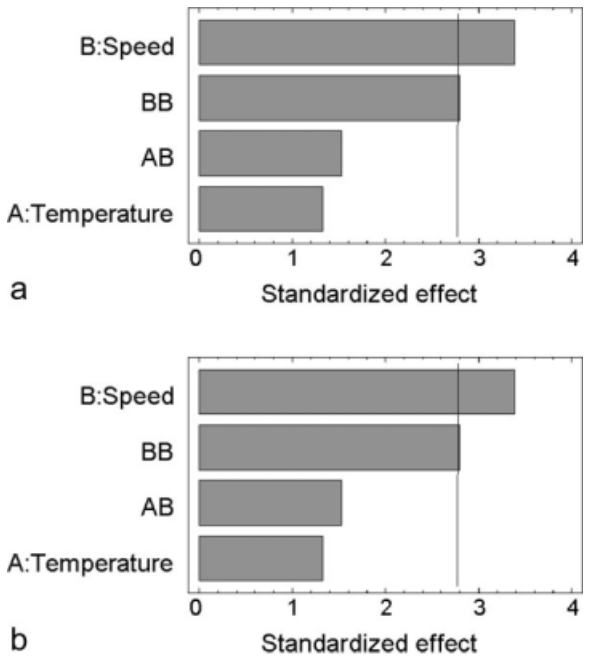

Figure 11 Pareto chart indicating the influencing factors and their combinations on (a) log (volume resistivity) and (b) macrodispersion index D of melt-mixed composites.

residence time, as it was found to be suitable in previous investigations using a Berstorff ZE25 extruder.[38]

Statistical analysis of the melt-mixing experiments based on the three levels, two-factor factorial experimental design was carried out to determine the main influencing factors affecting the resistivity [as log (volume resistivity)] and macrodispersion D.

The regression equations are as follows:

$$\begin{aligned}\mathrm{Log}_{10}[\text{volume resistivity}(\Omega\ cm)] &= -53.1678 + 0.295995 \times A(^{\circ}\mathrm{C}) + 0.0699972 \\ &\times B(\mathrm{rpm}) - 0.00165023 \times A \times B(^{\circ}\mathrm{C}, \mathrm{rpm}) \\ &+ 0.00132609 \times B^2(\mathrm{rpm}^2)\end{aligned}$$

$$\begin{aligned}\text{Macro dispersion index } D(\%) &= -36.7967 + 0.8385 \times B(\mathrm{rpm}) - 0.00145667 \\ &\times B^2(\mathrm{rpm}^2)\end{aligned}$$

The ANOVA leads to a correlation coefficient R^2 values of 84 and 99.5% for log (volume resistivity) and macrodispersion index D, respectively.

The estimated response surface charts in Figure 10(a) for $\log_{10}$ resistivity and in Figure 10(b) for the macrodispersion index D are 3D plots showing measured values and the model areas fitted using the regression equations of log (volume resistivity) and macrodispersion index D, respectively. These charts clearly indicate a general trend in resistivity and dispersion index D under varying mixing temperature and mixing speed.

From the fitted model shown in the estimated response surface chart of log (volume resistivity) as seen in Figure 10(a), an asymmetric "U"-shaped trend versus mixing speed can be seen, whereas a linear resistivity increase is fitted versus temperature at low speed and a slight decrease at high speed. In addition, some deviations of the measured points from the surface charts can be seen especially at low speed and low temperature, which is also reflected in the relatively low correlation coefficient of 84%. The shape represents the decrease in resistivity with mixing speed and the slight increases at maximum mixing speed as well as small differences at low temperature but big ones at high temperatures. The decrease in resistivity versus speed was expected as higher shear forces lead to better dispersion and distribution of MWNT agglomerates, whereas the unexpected trend of increase in resistivity at maximum speeds irrespective of mixing temperature may be attributed to the breakage of tubes and seems to be overestimated in the model.

From the fitted model shown in the estimated response surface chart of dispersion index [Fig. 10(b)], it can be seen that irrespective of mixing temperature, the dispersion index increases linearly with mixing speed.

Pareto charts indicate that for both log resistivity [Fig. 11(a)] and macrodispersion index D [Fig. 11(b)], only the factors speed (B) and square of the speed (BB) extend beyond the reference line. Thus, according to the model only these two factors show significant influence on resistivity and macrodispersion index D. However, it should be noted that the influence of mixing temperature as seen clearly in the resistivity values at 50 rpm seems to be not sufficiently reflected by the model.

To determine the percolation threshold of Baytubes in PC and to see the effect of optimized and nonoptimized mixing conditions, the Baytubes were compounded at two different mixing conditions. First, nonoptimized mixing conditions were used (265°C mixing temperature, 50 rpm mixing speed), and secondly after performing the variation in mixing conditions those leading to the best macrodispersion (macrodispersion index D is maximal) were applied (280°C mixing temperature, 200 rpm mixing speed); in both cases, mixing time was kept at 5 min.

The percolation threshold of Baytubes® C150HP in PC was determined on compression-molded plates by electrical resistivity measurements as illustrated in Figure 12. For the composites prepared at 265°C and 50 rpm, the percolation occurs between 0.5 and 1.5 wt %, whereas the composites mixed at 280°C and 200 rpm with smaller concentration steps

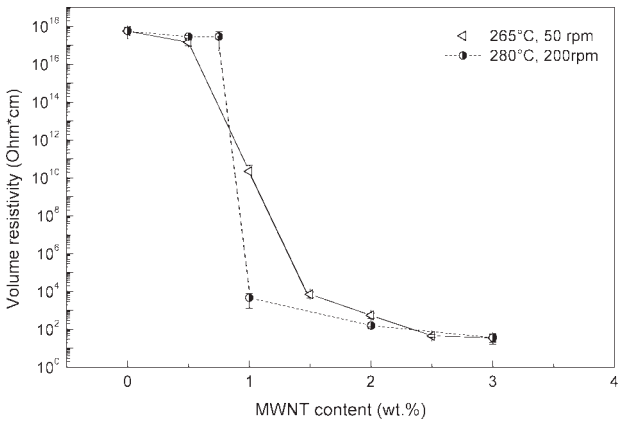

Figure 12 Percolation threshold of Baytubes® C150HP in polycarbonate composites produced under different mixing conditions.

indicated percolation between 0.875 wt % and 1 wt % MWNT. At 1 wt % MWNT content, the sample mixed at 265°C and 50 rpm shows much higher resistivity and is in the percolation range, whereas the sample prepared at 280°C and 200 rpm is already well percolated and conductive (resistivity $< 10^4$ Ω cm).

At concentrations higher or lower than the percolation concentration, no significant difference can be seen between both mixing conditions. This indicates that the electrical properties of composites with CNT are sensitive to processing conditions especially near the percolation concentration.

Variation of compression molding conditions

For studying the influence of compression molding parameters on the electrical volume resistivity near and above the percolation threshold, PC composites with 1 and 2 wt % MWNT were selected (see Fig. 12), which were produced in a kg scale using an extruder. The granules were compression molded by varying conditions such as pressing temperature, pressing time, and pressing speed using a three-level and three-factor factorial experimental design as described earlier.

In Figure 13(a,b), the effect of pressing time at different pressing conditions on the volume resistivity is shown for PC with 1 wt % MWNT.

At a pressing time of 1 min, resistivity decreases strongly with increasing temperature by almost 7–8 decades. Secondly, by increasing the pressing time at 260°C, resistivity decreases strongly. A decrease in resistivity with increasing time can also be observed at 280°C, whereas at 300°C, resistivity values remained nearly constant at quite low values of about 100–200 Ω cm over pressing time. It can be seen that pressing temperature followed by pressing time have strong influence on the restivity of these composites, whereas pressing speed has a low impact and does not show clear tendencies. At high temperatures, low pressing time is needed for low electrical resistivity, whereas at low melt temperatures, much longer time is needed to reach comparable states. The qualitative observations are similar to those described by Grossiord et al.[25] for the compression molding of PS–MWNT composites prepared by a latex approach where an equivalence of the impact of processing temperature and time was found.

The changes in resistivity during compression molding at different conditions can be assigned to a rearrangement in the nanotube network. Starting from a given state of small remaining MWNT agglomerates, small clusters, and individual tubes, the arrangement of these structural conductive elements and the polymer chains can be changed. Our results indicate that such a change or rearrangement of MWNT network needs very low time at low melt viscosity and thus quickly results in low resistivities.

Morphological investigations of selected pressed plates were carried out to investigate the structural changes that can cause lowering in resistivity. Optical micrographs of different pressed plates are

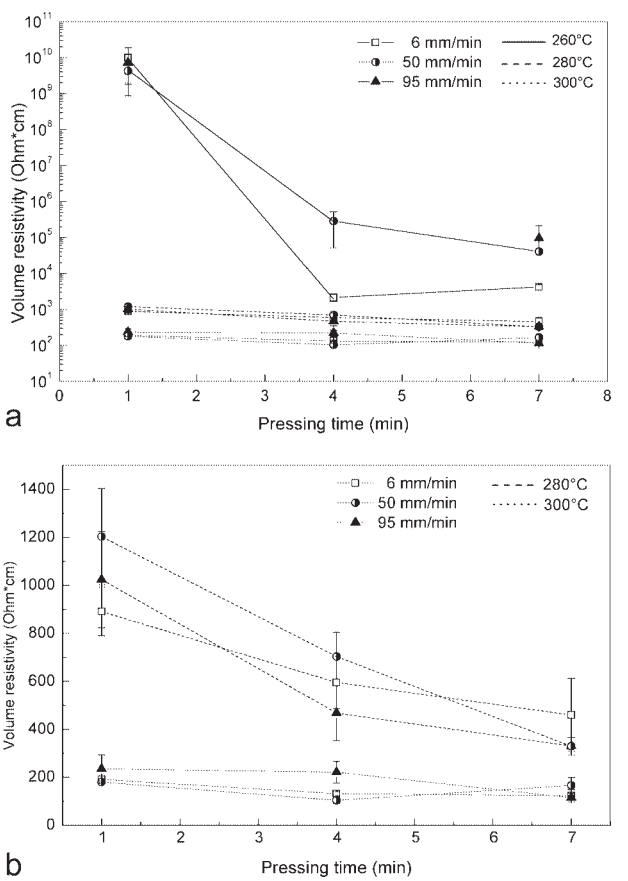

Figure 13 (a) Volume resistivity of PC + 1 wt % MWNT in dependence on pressing time and (b) magnification of (a).

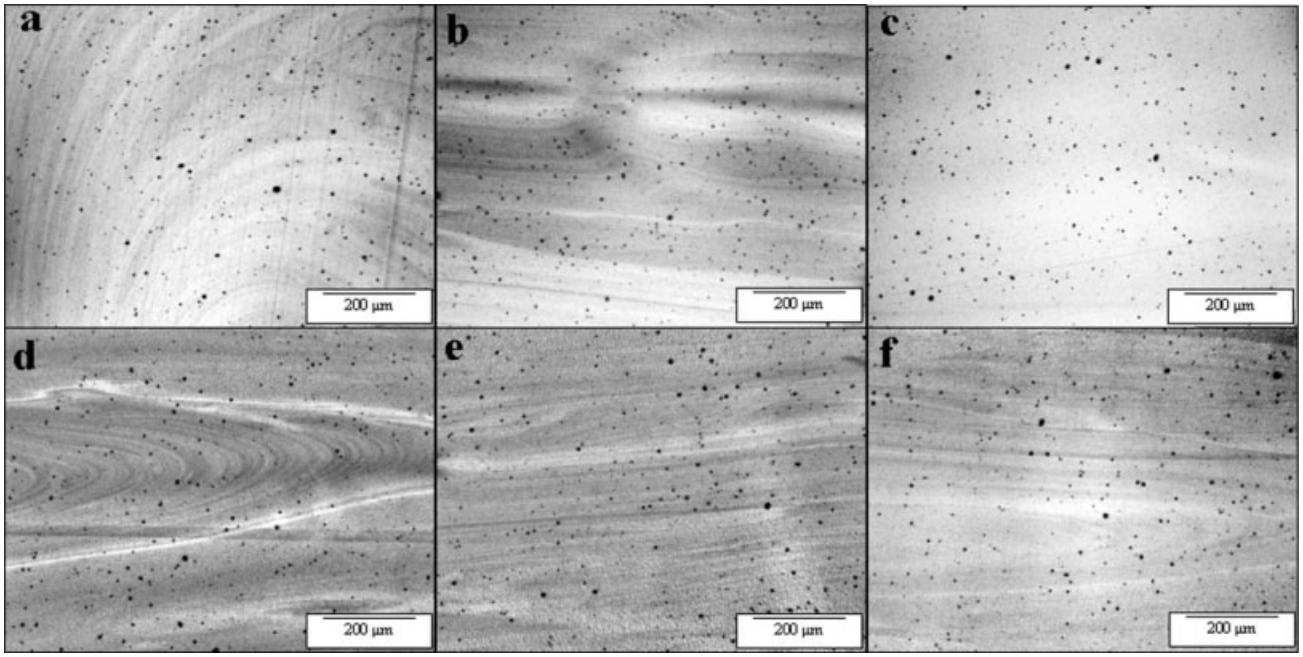

Figure 14 Optical micrographs of PC + 1 wt % MWNT samples under variation of pressing conditions: (a) as extruded composite; (b) 260°C, 6 mm/min, 1 min; (c) 260°C, 50 mm/min, 4 min; (d) 260°C, 50 mm/min, 7 min; (e) 280°C, 50 mm/min, 4 min; and (f) 300°C, 95 mm/min, 1 min.

exemplarily shown in Figure 14. It is obvious that no difference in agglomerate size and numbers (macrodispersion index: ~55%) can be seen among the samples as it was expected since no mixing takes place during compression molding. This indicates that probably the rearrangement of MWNT took place in the nanoscale.

Therefore, TEM investigations were performed on selected samples containing 1 wt % MWNT as shown in Figure 15, indicating clear differences in nanoscale morphology between the remaining primary agglomerates of these composites depending on the compression molding conditions. The starting granular sample as prepared by twin-screw extrusion [Fig. 15(a)] exhibits a good dispersion of mainly separated nanotubes. The good dispersion state of MWNT remains after compression molding at 260°C for 1 min [Fig. 15(b)], whereas at longer pressing time (4 min), the formation of some secondary nanoscale agglomerates of nanotubes is induced [Fig. 15(c)], resulting in the observed strong decrease of resistivity. Compression molding at 300°C and 7 min [Fig. 15(d)] leads to a stronger nanoscale agglomeration, and a network consisting of small loosely packed secondary agglomerates connected by separated MWNT is observed, which corresponds to the lowest resistivity values measured.

Thus, the lowering of resistivity can be explained by nanoscaled secondary agglomeration of MWNT in PC melt, which is enhanced with increasing compression molding temperature and time. The results presented here clearly indicate that the lowering in resistivity due to secondary agglomeration is a time-temperature-dependent process. Since pressing speed was shown to have only marginal influence, we assume that orientation of nanotubes in plate direction or formation of a frozen-oriented skin layer (as shown for injection molded samples[23]) are not dominant effects in these experiments.

Our results are in agreement with the viscosity- and time-dependent diffusivity and reorganization of MWNT in PS latex as mentioned elsewhere[25] and secondary agglomeration processes of individualized nanotubes as discussed earlier[18] and described in a model.[39] The results from this study have important impact on injection molding of MWNT-filled polymers, where especially the increase in melt temperature can be helpful in decreasing the resistivity of finished products.

To study the effect of compression molding conditions on volume resistivity of the percolated composite with 2 wt % MWNT, the same factorial experimental plan was applied. In Figure 16, volume resistivity versus pressing time at different pressing conditions is shown.

At this MWNT concentration, PC–MWNT composites are electrically percolated. Because of high loading of MWNT, the effect of different pressing condition is very low; however, similar tendencies can be observed as in case of PC + 1 wt % MWNT composites. Starting from resistivity values lower than 160 Ω cm, the differences in the resistivity

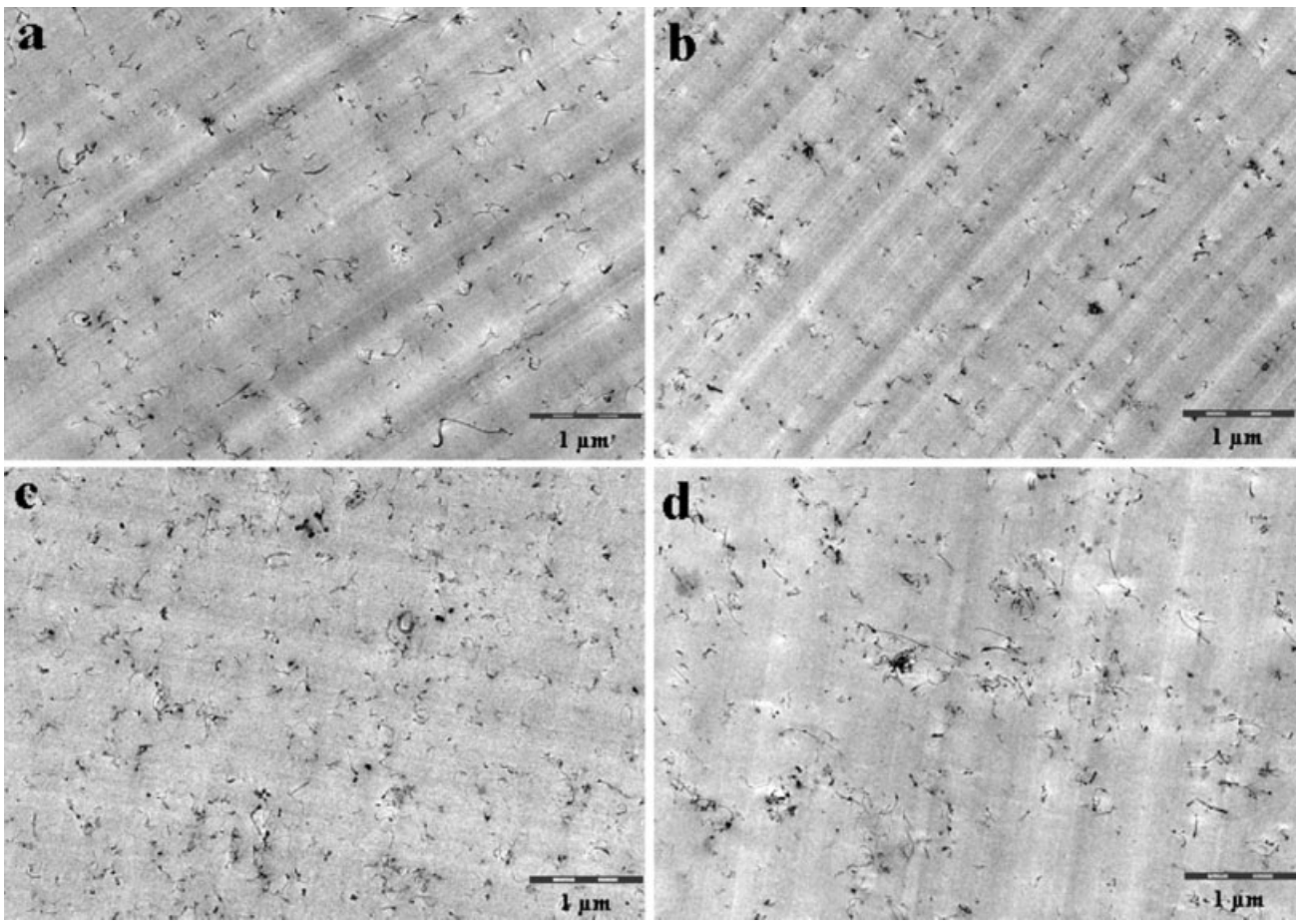

Figure 15 TEM micrograph of PC + 1 wt % MWNT samples under variation of pressing conditions: (a) as extruded composite; (b) 260°C, 1 min, 6 mm/min; (c) 260°C, 4 min, 6 mm/min; (d) 300°C, 7 min, 95 mm/min.

values are within one decade, thus secondary agglomeration probably also occurring here cannot reduce the resisitivity drastically.

To summarize, very high attention has to be paid when comparing the results of samples that are near the percolation threshold. Pressing conditions have to be mentioned as well as a judgment, if the measured values represent more likely a state near the initial one (as produced by mixing, preserved at low temperatures and less time) or a state near the equilibrium where resistivity has reached a minimum (at high temperatures and long time).

Statistical analysis of compression molding experiments, which are performed using a three-level and three-factor factorial experimental design, was carried out to determine influencing factors affecting the resistivity [as log (volume resistivity)].

The regression equations are as follows:

PC + 1 wt % MWNT :

$$\begin{aligned}\text{Log}_{10}[\text{volume resisitivity}(\Omega\ cm)] &= 405.091 - 2.66032 \times A(^{\circ}\text{C}) - 6.44611 \times C(\text{min}) \\ &+ 0.0043856 \times A^2(^{\circ}C^2) + 0.0218201 \times A \times C(^{\circ}\text{C}, \text{min})\end{aligned}$$

PC + 2wt % MWNT :

$$\begin{aligned}\text{Log}_{10}[\text{volume resisitivity}(\Omega\ cm)] &= 21.8971 - 0.127442 \times A(^{\circ}\text{C}) - 0.41715 \times C(\text{min}) \\ &+ 0.000197924 \times A^2(^{\circ}C^2) + 0.00139606 \times A \\ &\times C(^{\circ}\text{C}, \text{min})\end{aligned}$$

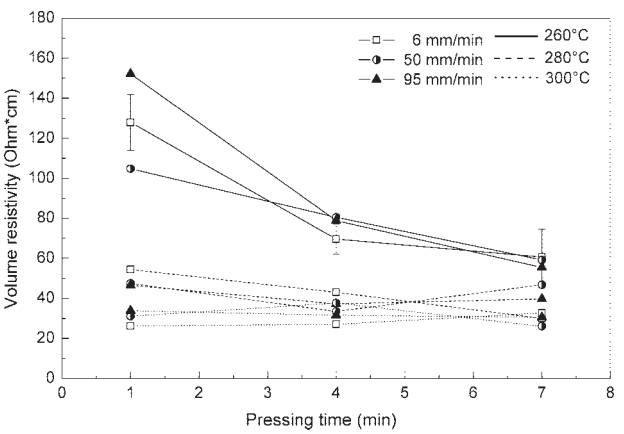

Figure 16 Volume resistivity of PC + 2 wt % MWNT compound in dependence on pressing time.

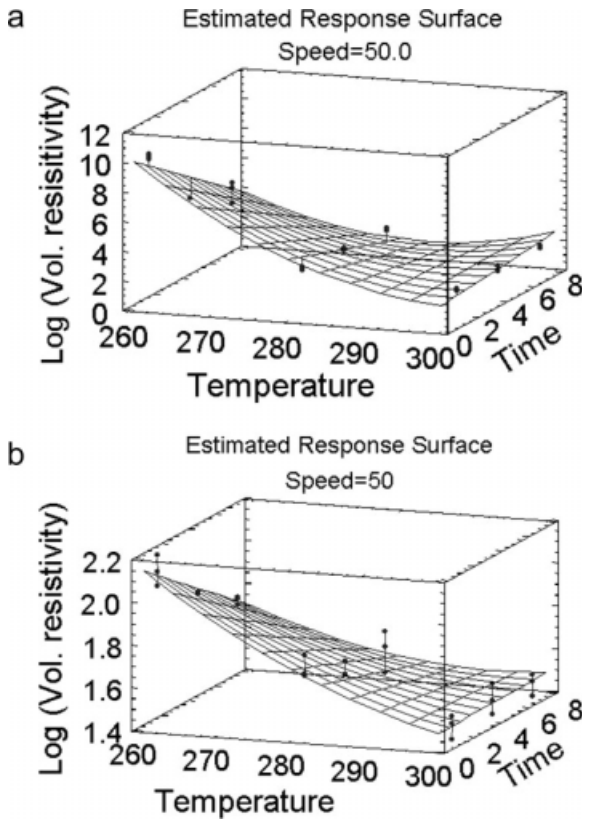

Figure 17 Estimated response surface chart of log (volume resistivity) for (a) PC + 1 wt % MWNT and (b) PC + 2 wt % MWNT in correlation with compression molding parameters.

The ANOVA leads to a correlation coefficient R^2 value of 92.2 and 93.8% for PC with 1 and 2 wt % MWNT, respectively.

The estimated response surface charts in Figure 17 are plotted at the reference pressing speed of 50 mm/min and indicate the general trend in log resistivity values along with the pressing temperature and time.

In both estimated response surface charts similar and clear tendencies can be seen, whereas as already discussed in PC + 1 wt % MWNT [Fig. 17(a)], resistivity changes are much larger when compared with PC + 2 wt % MWNT [Fig. 17(b)].

Trends in estimated response surface charts for PC + 1 wt % MWNT [Fig. 17(a)] indicate decrease in resistivity values as temperature increases, which seems to level off at higher temperature. At low temperature, a clear trend in reducing resistivity with pressing time is indicated, whereas at high temperature, no influence of pressing time is reflected. This also indicates that increasing pressing time above 7 min at 300°C will not help in decreasing the resistivity further and an asymptotic value of resistivity is reached. The low influence of pressing speed is reflected by the small deviation of the different measurement points from the area generated for 50 mm/min. From estimated response surface charts for PC + 2 wt % MWNT [Fig. 17(b)], the trends are quite similar as mentioned for PC + 1 wt % composites. The decrease in resistivity with temperature seems not to level off at 300°C, indicating that increasing the temperature above 300°C may marginally reduce the resistivity further.

The Pareto charts as shown in Figure 18 indicate for both MWNT amounts that the factors of compression molding temperature followed by the molding time and the product of temperature and time (or time-temperature interaction), as well as the square of the temperature, extend beyond the reference line indicating the significance of their influence on the resistivity of the composites. The Pareto charts indicate that for both composites pressing speed has no significant influence.

CONCLUSION

The electrical volume resistivity of PC–MWNT nanocomposites near the electrical percolation threshold concentration was found to be strongly influenced by processing conditions during melt mixing and compression molding.

In melt-mixed composites of polycarbonate containing 1 wt % MWNT Baytubes® C150 HP produced in a microcompounder at a fixed mixing time of 5 min, the variation of mixing temperature and mixing speed resulted in the variation of electrical volume resistivity between 10^{17} and 10^3 Ω cm. The mixing temperature influences the polymer melt

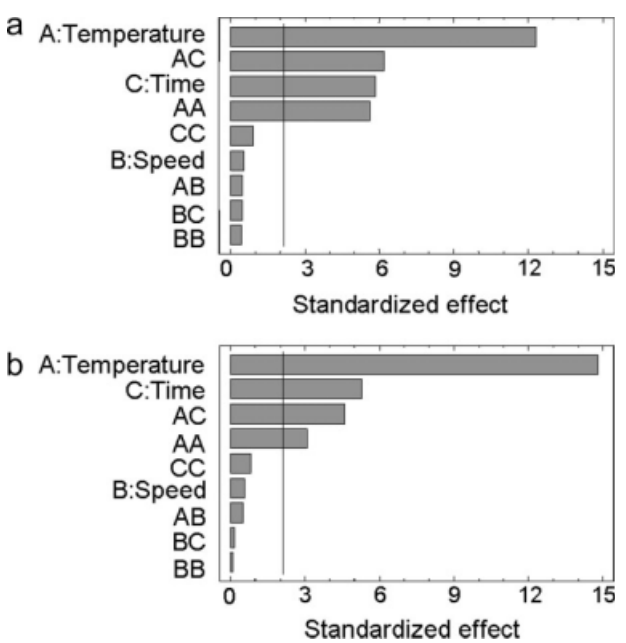

Figure 18 Pareto chart indicating the influencing compression molding factors and their combinations on log (volume resistivity) of (a) PC + 1 wt % MWNT and (b) PC + 2 wt % MWNT.

viscosity and therefore affects the required screw torque and mixing energy at a given rotation speed. It was observed that irrespective of the mixing temperature, the macrodispersion index D of MWNT agglomerates increases linearly with increasing mixing speed. A certain value of macrodispersion index D was found to be necessary to achieve low electrical volume resistivity. However, a higher dispersion index may not lead to lowering in resistivity. This means that comparable resistivity levels can be achieved at quite different states of nanotube dispersion. In context with the improvement in mechanical properties, samples without or with lower amount of remaining primary agglomerates are preferred. Nearly the same state of MWNT dispersion index and electrical resistivity can be achieved when incorporating the nanotube with high mixing speed either at high or low melt-mixing temperature, even if the mixing energy is much higher in the latter case. This indicates the differences in the dispersion mechanism of MWNT agglomerates and the state of network formation depending on the melt temperature. Mixing at low temperatures resulting in high shear stresses on MWNT agglomerates causes their dispersion mainly by agglomerate rupture, which in turns may damage the tubes with enhancing mixing speed. Here, the probability to form network structures consisting of agglomerates connected by dispersed tubes is higher. On the other hand, mixing at higher temperatures promotes the dispersion of MWNT agglomerates by erosion, and in combination with high mixing speeds, a balance can be achieved between rupture and erosion mechanism with less damage to the tubes. Here, more probably, network structures of finely dispersed tubes or by nanoscale secondary agglomeration are formed. Our results indicate that mixing at high melt temperature and high mixing speed can yield composites with low electrical volume resistivity and high macrodispersion index at relatively low mixing energy input.

In case of compression molding, strong impact of the compression molding parameters, molding temperature, and molding time on electrical volume resistivity was observed for composites with MWNT content near the electrical percolation concentration (here 1 wt %). Composites with resistivity varying from 10^{10} to 10^{2} Ω cm, i.e., either insulating or conductive samples were obtained by the variation in the compression molding parameters using the same precompounded MWNT composite. The lowering in resistivity by increasing either temperature or time is attributed to the secondary agglomeration of MWNT in the composite as also indicated in the TEM images and described by Pegel et al.[18] It seems that a certain lower limit in resistivity exists for a given MWNT concentration to which the values approach asymptotically and which cannot be undercut even when further increasing the molding temperature or time. It is an important outcome from this study that in scientific investigations attention has to be paid on the compression molding conditions, and there is a need to mention them in scientific reports to compare different results specifically for composites close to percolation threshold. For composites with higher MWNT concentration (above the percolation threshold), variations either in melt mixing or in compression molding have only marginal effect on the electrical resistivity values.

The authors thank Bayer MaterialScience AG, Leverkusen (Germany) for preparing and supplying the composites with 1 and 2 wt % Baytubes®, the Baytubes®C150HP, and helping in TEM investigations. They also thank Mr. Norbert Kendziorra from Continental AG for the statistical analysis of the resistivity and dispersion index results.

References

1. Iijima, S. Nature 1991, 354, 56.
2. Iijima, S. Mater Sci Eng B: Solid State Mater Adv Technol 1993, 19, 172.
3. Iijima, S.; Ichihashi, T.; Ando, Y. Nature 1992, 356, 776.
4. Raffaelle, R.; Landia, B.; Harris, J.; Bailey, S.; Hepp, A. Mater Sci Eng B 2005, 116, 233.
5. Wu, M.; Shaw, L. Int J Hydrogen Energy 2005, 30, 373.
6. Ago, H.; Petritsch, K.; Shaffer, M.; Windle, A.; Friend, R. Adv Mater 1999, 11, 1281.
7. Hidden, G.; Boudou, L.; Remaurya, S.; Nabarraa, P.; Martinez, J. J Optoelectron Adv Mater 2004, 6, 1065.
8. Varghese, O.; Kichambre, P.; Gong, D.; Ong, K.; Dickey, E.; Grimes, C. Sens Actuators B chem 2001, 81, 32.
9. Philip, B.; Abraham, J.; Chandrasekhar, A.; Varadan, V. Smart Mater Struct 2003, 12, 935.
10. Wang, Q.; Setlur, A.; Lauerhaas, J.; Dai, J.; Seelig, E.; Chang, R. Appl Phys Lett 1998, 72, 2912.
11. Kim, H.; Kim, K.; Lee, C.; Joo, J.; Cho, S.; Yoon, H.; Pejakovic, D.; Yoo, J.; Epstein, A. Appl Phys Lett 2004, 84, 589.
12. Ma, C.; Huang, Y.; Kuan, H.; Chiu, Y. J Polym Sci Part B: Polym Phys 2005, 43, 345.
13. Yang, Y.; Gupta, M.; Dudley, K.; Lawrence, R. J Nanosci Nanotechnol 2005, 5, 927.
14. Fan, Z.; Luo, G.; Zhang, Z.; Zhou, L.; Wei, F. Mater Sci Eng B 2006, 132, 85.
15. Hagerstrom, J.; Greene, S. Commercialization of Nanostructured Materials Conference Proceedings, Miami, Florida, April 6–7, 2000.
16. Ferguson, D.; Bryant, E.; Fowler, H. ANTEC 1998, 98, 1219.
17. Pötschke, P.; Bhattacharyya, A.; Janke, A.; Pegel, S.; Leonhardt, A.; Täschner, C.; Ritschel, M.; Roth, S.; Hornbostel, B.; Cech, J. Fullerenes Nanotubes Carbon Nanostruct 2005, 13, 211.
18. Pegel, S.; Pötschke, P.; Petzold, G.; Dudkin, S.; Lellinger, D.; Alig, I. Polymer 2008, 49, 974.
19. Lin, B.; Sundararaj, U.; Pötschke, P. Macromol Mater Eng 2006, 291, 227.
20. Lellinger, D.; Xu, D.; Ohneiser, A.; Skipa, T.; Alig, I. Phys Stat Sol B 2008, 245, 2268.
21. Pötschke, P.; Fornes, T.; Paul, D. Polymer 2002, 43, 3247.
22. Pötschke, P.; Dudkin, S.; Alig, I. Polymer 2003, 44, 5023.
23. Villmow, T.; Pegel, S.; Pötschke, P.; Wagenknecht, U. Compos Sci Technol 2008, 68, 777.

24. Krause, B.; Pötschke, P.; Häußler, L. Compos Sci Technol, doi: 10.1016/j.compscitech.2008.07.007.
25. Grossiord, N.; Kivit, P.; Loos, J.; Meuldijk, J.; Kyrylyuk, A.; van der Schoot, P.; Koning, C. Polymer 2008, 49, 2866.
26. Bayer Material Science Baytubes C150HP, Bayer Material Science Datasheet; Bayer MaterialScience AG: Germany.
27. Pötschke, P.; Goad, M.; Alig, I.; Dudkin, S.; Lellinger, D. Polymer 2004, 45, 8863.
28. Stumpe, N.; Railsback, H. Rubber World 1964, 151, 41.
29. Le, H.; Ilisch, S.; Prodanova, I.; Radusch, H. Kautsch Gummi Kunstst 2004, 57, 355.
30. Radusch, H.; Le, H.; Ilisch, S.; Kasaliwal, G. Fibre Reinforced Composites Conference; Port Elizabeth, South Africa, December 9–12, 2007.
31. Kasaliwal, G. MSc Thesis, Centre of Engineering Science, Martin Luther University, Germany, 2007.
32. Medalia, A. J Colloid Interface Sci 1970, 32, 115.
33. Box, G. E. P.; Stuart Hunter, J.; Hunter, W. G.Statistics for Experimenters: Design, Innovation, and Discovery; Wiley: New York, 2005.
34. Duncan, A. J. Quality Control and Industrial Statistics; 4th ed.; Irwin: Homewood, IL, USA, 1986.
35. Antony, J. Design of Experiments for Engineers and Scientists; Elsevier Science & Technology Books: October 2003. ISBN 0750647094.
36. Andrews, R.; Jacques, D.; Minot, M.; Rantell, T. Macromol Mater Eng 2002, 287, 395.
37. Fan, Z.; Advani, S. J Rheol 2007, 51, 585.
38. Villmow, T.; Pötschke, P.; Pegel, S.; Häussler, L.; Kretzschmar, B. Polymer 2008, 49, 3500.
39. Alig, I.; Skipa, T.; Lellinger, D.; Pötschke, P. Polymer 2008, 49, 3524.